Activation of hTREK-1 by polyunsaturated fatty acids does not only involve membrane tension

Emilie BECHARD[1], Elodie AREL[1], Jamie BRIDE[1], Julien LOURADOUR[1], Xavier BUSSY[1], Anis ELLOUMI[2], Claire VIGOR[2], Camille OGER[2], Jean-Marie GALANO[2], Thierry DURAND[2], Jean-Yves LE GUENNEC[$,1], Marie DEMION[$,1].

[1]: PhyMedExp, Université de Montpellier, Inserm U1046, UMR CNRS 9412Montpellier (France)
[2]: IBMM, Université de Montpellier, UMR CNRS 5247, ENSCM, Montpellier (France)

[$] Co-corresponding authors

Marie DEMION
PhyMedExp, Inserm U1046, CNRS UMR9214
CHU Arnaud de Villeneuve
Bâtiment Craste de Paulet
370 avenue du Doyen Gaston Giraud
34290 MONTPELLIER Cedex 05
France

Jean-Yves LE GUENNEC
PhyMedExp, Inserm U1046, CNRS UMR9214
CHU Arnaud de Villeneuve
Bâtiment Craste de Paulet
370 avenue du Doyen Gaston Giraud
34290 MONTPELLIER Cedex 05
France

Running title : hTREK-1 is directly activated by PUFAs

ABSTRACT

Among two-pore domains K^+ channels, twik-related K^+ channels (TREK) are characterized by a polymodal activation including membrane stretch and polyunsaturated fatty acids (PUFAS). So far, there is no systematic comparison of PUFAs activation on I_{TREK-1} and no clear reliable action mechanism.

In this study, we performed a thorough comparison of the effects of fatty acids (FA) having between 18 and 22 atoms of carbon and 0 to 6 double bonds and ML402, a well-known direct activator of TREK-1. We observed no relationship between acyl chain length and/or number of double bonds and TREK-1 activation. This suggests that the bilayer-couple hypothesis cannot explain by itself all the activation of TREK-1 by PUFAs. We found that the two strongest activators are linoleic acid and docosahexaenoic acid, respectively the shortest with two double bonds and the longest with six double bonds PUFAs. We also found that the important variability of I_{TREK-1} activation by PUFAs is related to the variable constitutive activity of TREK-1. Based on activation and washout kinetic analysis using two configurations of patch-clamp, we propose that PUFAs activate TREK-1 mainly following a direct interaction with the channel.

INTRODUCTION

Potassium channels have a crucial role in the electrical activity of excitable cells such as neurons and cardiomyocytes. Some of these potassium channels are common drugs targets modulating the action potential shape and consecutively organs functions. Among the K^+ channels, members of the two-pore domains K^+ channels family (K2P) are involved in the repolarization phase of action potential and in the resting membrane potential (Kelly *et al*, 2006). K2P family includes 15 members classified in 6 functional subfamilies: TWIK (**T**andem of pore domains in a **W**eak **I**nward rectifying **K** channel), TREK (**T**WIK-**Re**lated **K**

channel), TASK (**T**WIK-related **A**cid **S**ensitive **K** channel), TALK (**T**WIK-related **Al**kaline pH-activated **K** channel), THIK (**T**andem pore domain **H**alothane-**I**nhibited **K** channel), TRESK (**T**WIK-**Re**lated **S**pinal Cord **K** Channel). K2P channels share common structural features, each subunit containing two-pore domains (P1, P2) and four putative transmembrane segments (M1-M4)(Honoré, 2007). The dimerization of K2P channels allows the formation of the canonical K^+ selective pore domain. TREK-1 channel, one of the three members of the TREK subfamily along with TREK-2 and TRAAK, has been discovered in 1996 by Fink *et al*. The gating of TREK-1 channel is poly-modulated by a wide range of physical and chemical stimuli including mechanical stretch, temperature, voltage, pH, pharmacological agents and polyunsaturated fatty acids (PUFAs). This channel is widely studied since its activation is involved in neuroprotection (Lamas & Fernández-Fernández, 2019), cardioprotection (Kamatham *et al*, 2019), analgesia (Li & Toyoda, 2015) and reduced epilepsy crisis (Heurteaux *et al*, 2004). In the majority of these diseases, the protection afforded by TREK-1 activation is due to the hyperpolarization of the membrane potential (Djillani *et al*, 2019)

Among the wide diversity of TREK-1 modulators, PUFAs have been shown to behave as strong activators (Patel *et al*, 1998; Danthi *et al*, 2003). PUFAs are classified according to their structure and consist of carboxylic acids with a long chain of carbons and multiple double bonds. The two main classes of PUFAs are n-3-PUFAs and n-6-PUFAs based on the position of the first double bond from the carbon ω starting at the methyl extremity. Numerous studies suggest that n-3-PUFAs, such as docosahexaenoic acid (DHA) and eicosapentaenoic acid (EPA), exert antiarrhythmic properties through the modulation of ionic channels and consequent membrane hyperpolarization (Kang & Leaf, 1994, 1996). Such hyperpolarization could be consecutive to TREK-1 activation. TREK channels are mechano-sensitives and a comparison of the effects of different PUFAs on TRAAK suggests that

PUFAs can insert inside the membrane (Fink *et al*, 1996) inducing an increase in membrane fluidity (Leifert *et al*, 1999) that in turn modifies membrane tension. TRAAK is very likely to be activated by PUFAs through this mechanosensitive pathway since the activation is related to the acyl chain length and to the number of double bonds (Maingret *et al*, 1999; Honoré, 2007). While it has also been inferred that the same applies to TREK-1, there is no study to date that compared the effects of different PUFAs on TREK-1.

To better understand the mechanism of action of PUFAs activating TREK-1, we performed a thorough comparison of the effects of 8 PUFAs (from 18 to 22 carbons with 2 to 6 double bonds) and 2 other C18 FA (mono-unsaturated and saturated) on the TREK-1 current (I_{TREK-1}). The effects were compared to those obtained with ML402 application, a direct activator of TREK-1 binding within a cryptic pocket behind the selectivity filter that directly stabilize the C-type gate (Lolicato *et al*, 2017).

RESULTS

TREK-1 channel activation by PUFAs

As previously described by others, TREK-1 channel is activated by PUFAs, such as arachidonic acid (AA) (Patel *et al*, 1998), LA (Danthi *et al*, 2003) or DHA (Ma & Lewis, 2020). In resting conditions, the average membrane potential (Em) of hTREK-1/ HEK was -69.2 ± 0.7 mV (mean ± SEM) (n=130, 95% CI = [-67.8; -70.6]), with a variable current density of 15.3 ± 1.2 pA/pF (n=130, 95% CI = [13.0 ;17.6]) at 0 mV. During PUFAs or ML402 10 µM superfusion (see structures on **Fig 1**), the current density progressively increased until a steady-state was reached (**Fig 2A**, illustration of I_{TREK-1} activated by DHA). When TREK-1 is activated, Em hyperpolarized to -81.7 ± 0.3 mV (n=130; 95% CI = [-81.2; -82.3]), close to the theorical equilibrium potential for K^+ ion (E_{K+} = -86 mV).

To compare the responses of each compound, we plotted the current density at 0 mV in the presence of PUFAs or ML402 normalized to the initial current density (I_0) that corresponds to the current fold-increase (I_{PUFA}/I_0). As shown in **Fig 2B** and **Table 1**, all PUFAs but ALA increased I_{TREK-1}. The activation sequence of tested compounds was: LA ~ DPA n-6 ~ DHA > ETA n-3 ~ ETA n-6 ~ EPA ~ DPA n-3 ~ ML402. Like ALA, the saturated stearic acid (C18:0) had no effect on I_{TREK-1} while the mono-unsaturated oleic acid (C18:1n-9) produced a 7.4 ± 1.9-fold increase of I_{TREK-1} (n=12, **Table 1**). Comparing the effects of PUFAs, based on their series, revealed that there was no relationship neither with the length of the acyl chain within series nor with the number of double bonds and the effect on I_{TREK-1}. Indeed, DHA (C22:6 n-3) tended to have a stronger effect than DPA n-3 (C22:5 n-3) while they share the same number of carbon (**Fig 2C**). Accordingly, the most potent activators among the n-6 PUFAs were both the shortest one, LA and the longest one, DPA n-6 having 2 and 5 double bonds respectively (**Fig 2D**). These results suggest that TREK-1 activation by PUFAs is not due to their acyl chain length nor their number of double bonds. However, the statistical

analysis of the sequence shows no differences between the PUFA's effects. This lack of apparent differences is likely due to an important variability of the effects. Despite an important number of cells studied, we observed a large variability of I_{TREK-1} activation by PUFAs (**Table 1**). The severity of the inclusion criteria (see Material and Methods section) suggests that the variability observed is inherent to TREK-1 channel.

The variability in PUFAs responses is related to the variable initial current density

We observed that the basal current (I_0) varied and might influence the degree of activation of I_{TREK-1} in response to PUFAs. This variability of I_0 reflects different levels of constitutive activation of TREK-1 channel. **Fig 3A** illustrates the huge variability of PUFAs effects based on the fold-increase analysis (I_{PUFA}/I_0) depending on I_0. We focused our analysis on I_{PUFA} to discriminate statistically the PUFA's effects. We observed that the current density tended to a maximal I_{PUFA} specific for each PUFAs with a reduced dispersion compared to current fold-increase I_{PUFA}/I_0 (**Fig 3B)**. This was confirmed by calculating the coefficient of variation (CV $= \frac{SD}{Mean}$) as CV decreased for I_{PUFA} compared to I_{PUFA}/I_0 (**Fig 3C**). Therefore, CV modification is in accordance with the hypothesis that PUFAs tend to activate TREK-1 channels from a variable I_0 to a maximal current density. In contrast to PUFAs, ML402 response did not induce response variability (**Fig 3A**). Indeed, the SD and the CV increased for I_{ML402} suggesting that there is no link between ML402 response and the initial current density (**Fig 3B and C, Table 2**).

To better characterize the dependence between I_0 and I_{PUFA}, we plotted the fold-increase of I_{TREK-1} current (I_{PUFA}/I_0 and I_{ML402}) *versus* the initial current (I_0). As shown in **Fig 4A,** there is a non-linear relationship between I_{PUFA}/I_0 and I_{ML402} *versus* I_0. However, this relationship can be linearized by log-transforming the data (Log10) (**Fig 4B**). Independently of the absolute amplitude of I_{PUFA}, this transformation reveals that the effects of all PUFAs but DPA n-3

146 (R^2=0.08, p-value=0.37) depends on I_0. Therefore, there is a negative correlation between
147 Log10(I_{PUFA}/I_0) and Log10(I_0) for LA (R^2=0.82), ETA (R^2=0.80), AA(R^2=0.50), EPA
148 (R^2=0.53), DPA n-6 (R^2=0.84) and DHA (R^2=0.68)(**Table 3**). In conclusion, the current fold-
149 increase variability with PUFAs observed can be explained by the varying constitutive
150 activity of TREK-1 channel.
151 Thanks to the linear regression, we obtained the Y-intercept that reflects the fold activation of
152 I_{TREK-1} for a unitary current (Log(1)=0). The Y-intercept gives the following sequence of
153 activation : LA ~ DHA ~ DPA n-6 ~ ETA n-6 > ETA n-3 ~ EPA. This sequence, closed to
154 that of I_{PUFA}/I_0, is however based on a statistical linear regression. The Y-intercept of DPA n-
155 3 and ML402 could not be calculated since there was no correlation.
156
157 **Fast and slow activation kinetics according to PUFAs**
158 To better understand the mechanism(s) of action of PUFAs on TREK-1 channel activation
159 (fast or delayed), we analyzed the kinetic of I_{TREK-1}. **Fig 5A** shows typical time courses
160 obtained by plotting the normalized current densities (($I-I_0$)/($I_{PUFA}-I_0$)). The activation rate
161 was calculated using the inverse of the time constant τ (**Fig 5B**). We were able to distinguish
162 at least two types of activation rate, a fast one more than 3 min^{-1} (LA, DHA, ML402, EPA)
163 and a slow one less than 3 min^{-1} (ETA n-3, ETA n-6, DPA n-3). As reported in **Table 4**, the
164 averaged half-activation of TREK-1 channel were faster for LA and DHA, both having
165 kinetics comparable to ML402. Although there was no significant differences between these
166 three compounds and DPA n-6 and EPA, the kinetics of the latters appeared slightly slower
167 (**Fig 5B, Table 4**). In contrast, ETA n-3, ETA n-6 and DPA n-3 had a slower kinetic with an
168 averaged half-activation closed to 4 min (**Table 4**).
169 All these data suggest a possible direct interaction between PUFAs and TREK-1. To confirm
170 it, we looked at the washout kinetic as it should not be washable if the effect is only due to

171 membrane insertion. We focused on LA, EPA and DHA, the most potent activators of C18,
172 C20 and C22 PUFAs respectively. ML402 activation reversed immediately and 50% of
173 washout occurred in less than 1min (**Fig 6, Table 5**). Even though the washout was slower,
174 PUFAs activation were also reversed under washout with a simple bath solution. EPA, that
175 activated TREK-1 in the same magnitude than ML402, had a kinetic of washing comparable
176 to ML402. LA and DHA, that activated TREK-1 at least twice more than ML402, had
177 kinetics of washout slower even though it was complete in few minutes. At this point, we do
178 not exclude a membrane insertion of PUFAs, that might explain the longer time of washing of
179 DHA, but we assume that the main effects of PUFAs are due to a direct and reversible
180 interaction of PUFAs with the channel.
181
182 **Activation of I_{TREK-1} by PUFAs and ML402 in inside-out configuration**
183 In order to deepen the direct interaction hypothesis, we used the inside-out configuration of
184 the patch-clamp technique. In this configuration, we were able to superfuse molecules at the
185 inner face of the membrane. As shown in **Fig 7A**, ML402 superfusion at the inner face of the
186 membrane induced a reversible increase of I_{TREK-1} (**Table 6**). Kinetics of activation and
187 washout were comparable to those obtained in the whole-cell configuration (**Fig 5 and 6**)
188 suggesting that the ML402-binding site is accessible from the outside and the inside of the
189 cell. Interestingly, a comparable reversible activation of TREK-1 was obtained for LA and
190 DHA (**Fig 7B and 7C**) while PUFAs-induced curvature of the membrane is supposed to not
191 be the same when PUFAs are applied fat the inner or the outer bilayer of the cell membrane.
192
193
194 **DISCUSSION**
195 **TREK-1 channel activation by PUFAs**

In this study, we reported that TREK-1 channel is reversibly activated by polyunsaturated fatty acids (PUFAs), as already shown in different studies each being focused mainly on one PUFA : AA (Patel *et al*, 1998); LA (Danthi *et al*, 2003); DHA (Ma & Lewis, 2020). Our study is the first to compare the effects of different PUFAs having between 18 to 22 carbon atoms and 2 to 6 double bonds on TREK-1 channel. We demonstrate that DHA (C22:6n-3) and LA (C18:2n-6) are the most potent activators of TREK-1 with activation as fast as the one of the direct activator ML402. TREK subfamily of K2P channels, that includes TREK-1, TREK-2 and TRAAK, is characterized by a mechano-sensitivity and therefore, the channels can feel changes in the membrane curvature induced by PUFAs insertion. As PUFAs are anionic amphipath compounds, with a hydrophilic carboxyl group and a hydrophobic tail, they preferentially insert into the outer leaflet of the membrane which is positively charged (Martinac *et al*, 1990; Sheetz & Singer, 1974). Thus, the longer the carbon chain is (hydrophobic tail), the more the PUFAs will be inserted into the membrane, modifying the membrane curvature and fluidity. Also, for a given acyl chain length, the membrane fluidity increases with the number of double bonds. According to the bilayer-couple hypothesis, PUFAs effects on TREK subfamily channels were supposed to be due to an interaction within the membrane leading to an increase of the tension transmitted to the channels (Patel *et al*, 1998). The study of the TRAAK channel activation by PUFAs (C18:2n-6, C20:4n-6, C20:5n-3, C22:6n-3) in the excised patch configuration indicates that I_{TRAAK} activation is positively correlated with the tail length of PUFAs and the number of double bonds (Fink *et al*, 1998; Patel *et al*, 2001). However, in our model of overexpressing HEK-293/hTREK-1 cell line, we found no correlation between the acyl chain length, the number of double bonds and the potentiation of I_{TREK-1}. In the opposite, LA and DHA, respectively the shortest and the longest PUFAs, are the most potent activators of TREK-1 channel. It is worth to note that ALA (C18:3n-3), which differs only by one double bond from LA, failed to activate TREK-1

channel. PUFAs having intermediate chain length produce intermediate activation of TREK-1, independently of the double bonds number. Similar results were obtained in the literature on TREK-2 channel study, AA being less efficient than DHA and LA (Lesage *et al*, 2000). In that respect, the bilayer-couple hypothesis suggesting an activation of the channels by PUFAs insertion is not appropriate for TREK-1 since it has been shown that the membrane fluidity, and so membrane tension, increases with the acyl chain length (Leifert *et al*, 1999).

Studies have already hypothesized that arachidonic acid could act directly by interacting with the channel (Maingret *et al*, 1999, 2000). To understand the mechanism of action of DHA and LA on I_{TREK-1}, we compared their effects with those of ML402, a well know activator of TREK-1 channel. ML402 is a direct activator of TREK-1, binding within a cryptic pocket behind the selectivity filter that directly stabilize the C-type gate (Lolicato *et al*, 2017). The activation kinetic of I_{TREK-1} by DHA, LA and ML402 are comparable and faster than the other PUFAs. This suggests a direct binding of DHA and LA to the channel like the inhibitor norfluoxetine (Dong *et al*, 2015) and the activator ML402 (Lolicato *et al*, 2017). This is reinforced by the inside-out experiments where DHA, LA and ML402 were applied on the inner side of the membrane. Although the PUFAs insertion must induce opposite curvartures while they insert from the inner or the outer layer, they still activate TREK-1 channel in the same way. We finally propose that at least DHA and LA, like ML402, interact with the channel on an accessible site from both the inside and the outside of the cell membrane. The steady-state of TREK-1 activation by PUFAs and ML402 was reached in the range of the minutes suggesting that the binding-sites have a limited access (Maingret *et al*, 2000). Moreover, it has to be noted that bovine serum albumin (BSA) is not required to get a reversal effect during the washout as it is supposed to be when the effects are due to membrane insertion of the PUFAs (Kang & Leaf, 1994; Leifert *et al*, 1999). Moreover, in both whole-cell and inside-out configurations, the washout kinetics of PUFAs were immediate and the

initial current recovered in few minutes. However, despite a total washout, we cannot exclude a membrane insertion of the PUFAs as washout were longer for DHA and LA when compared to ML402 in whole-cell recording. Therefore, we propose that both mechanisms, PUFAs insertion into the membrane and direct binding to TREK-1 channel, act together to increase I_{TREK-1}, since increasing the membrane fluidity by PUFAs insertion should facilitate the access to their binding site.

Basal TREK-1 variability influence PUFAs response

An unexpected result of this study is the observation that the PUFAs effects depend on the basal current, carried mainly by TREK-1 channel. However, independently of the basal activity of TREK-1, a maximal conductance is finally reached. This suggests TREK-1 conductance is activated toward a value linked to the PUFA itself. This variability in basal I_{TREK-1} might have many origins such as different levels of post-translationnal modifications, differences in membrane tension between cells or even the presence of 2 different conductances of TREK-1 channel at the single channel level (Xian Tao Li *et al*, 2006). A comparable variability in the current-fold increase induced by PUFAs was already observed for TREK-1 activation by AA (Maingret *et al*, 2000), TRAAK (Fink *et al*, 1998; Patel *et al*, 2001) and TREK-2 (Bang *et al*, 2000; Lesage *et al*, 2000) but never explained. At this time, it would be interesting to check if this variable response is also related to the variability of the basal current. It is important to note that all these works were performed on COS-7 cells or HEK-293 cells where mammalian post-translational modifications exist. In the study of Ma and Lewis in 2020, whole-cell recording of I_{TREK-1} and I_{TREK-2} activated by arachidonic acid were performed in oocytes (*Xenopus Laevis*) and no such variability in the current fold-increase was observed. It is known that in this heterologous expression model, post-translational modification are different (Mantegazza *et al*, 2010). Therefore, the possibility

that constitutive I_{TREK-1} varies according to the phosphorylation level (or other modifications) and influence the effects of PUFAs should be taken in consideration. It is known that TREK-1 channel is modulated by intracellular pathways, related to PKA, PKC and PKG signalizations (Koh *et al*, 2001; Murbartián *et al*, 2005; Honoré, 2007), but to the best of our knowledge, no study between PUFAs activation of TREK-1 and phosphorylation levels has been performed so far. Such a link might exists and explains that ML402 activation of TREK-1 is independ of the constitutive I_{TREK-1}. Whatever the variability of constitutive I_{TREK-1} originates from, this result clearly indicates that the analysis of I_{PUFA}/I_0, or fold-increase of I_{TREK-1}, is not acurate. A sufficient number of studied cells has to be investigated and the Y-intercept of the regression line is probably the best indicator of the degree of activation of I_{TREK-1}. The existance of such variability should be taken into consideration in pathophysiological studies associated with variability of expression or response, potentially demultiplying the heterogeneity of TREK-1 response to activators.

Surprisingly, the most efficient activator of TREK-1 channel is LA. This suggests that LA displays potent cardio- and neuroprotective effects. As TREK-1 is expressed in cardiomyocytes (Li & Toyoda, 2015; Kelly *et al*, 2006; Decher *et al*, 2017) LA should modulate action potential shape and resting membrane potential. If anti-arrhythmic properties of omega-3 FA have been thoroughly studied (Kang & Leaf, 1994, 1996; Siscovick *et al*, 2017), the potential anti-arrhythmic effect of omega-6 FA such as LA has never been considered. LA can be found in vegetarian and Mediterranean diets, both diets having cardioprotective vertues (de Lorgeril *et al*, 1994; Barnard *et al*, 2019). In both cases the beneficial effects are attributed to the presence of anti-oxidant molecules and ALA but a possible beneficial effect of LA has never been explored.

295 To conclude, there is no relationship between the carbon number of the acyl chain, the
296 number of double bonds and the activation of TREK-1. The most potent activators of TREK-1
297 are LA and DHA and the comparison of the kinetics of activation and of washout with those
298 of ML402 suggests a direct activation of TREK-1. This direct activation of TREK-1 by
299 PUFAs could be combined with the membrane insertion of PUFAs to facilitate the access to
300 the binding site on the channel. The variability of I_{TREK-1} in basal conditions influences the
301 fold-increase activation while the maximum activation of I_{TREK-1} by PUFAs tends toward
302 values characteristics of each PUFA.
303
304
305 **MATERIEL AND METHODS**
306
307 **Cell culture**
308 We used a HEK-293 cell line that stably expresses the human TREK-1 channel subunit
309 (Moha ou Maati *et al*, 2011). Human-TREK-1/ HEK cells were grown in an atmosphere of
310 95% air/5% CO_2 in Dulbecco's modified Eagle's medium and Glutamax (Invitrogen, Cergy-
311 Pontoise, France) supplemented with 10% (v/v) heat inactivated fetal bovine serum and 1%
312 (v/v) penicillin/streptomycin and 0.5mg/mL G418 to maintain a selection pressure.
313
314 **Electrophysiology**
315 Currents were recorded from hTREK-1/HEK-cells using the patch-clamp in whole-cell
316 recording (WCR) configuration and in inside-out (IO) configuration. Patch pipette having 2.5-
317 4 MΩ resistances (WCR) and 5-7 resistances (IO) were obtained from borosilicate glass
318 capillaries by using a two-stage vertical puller (PC- 10, Narishige, London, UK). Current
319 acquisition was performed with an Axopatch 200B amplifier (Axon Instrument, Sunnyvale,

320 CA, USA) and low-pass filtered at 5 kHz (WCR) and 2 kHz (IO). Data were digitalized with a
321 digidata 1550B (Axon Instrument, Sunnyvale, CA, USA) at 10 kHz. The pClamp10.7 (Axon
322 Instrument) software was used to impose stimulations protocols and record TREK-1 current.
323 In WCR, cells were kept for experiments if the series resistance were lower than 8 MΩ, the
324 membrane capacitance between 20 and 35 pF.
325 The experiments were performed at room temperature (~22 °C). Cells were continuously
326 superfused with a bath solution and modulatory compounds at a rate of 1-1.5 mL/min. The
327 dishes volume was kept constant at 2.5-3 mL using a vacuum system, connected to a
328 peristaltic pump (ISMATEC). Using different extracellular potassium concentrations (5 mM
329 KCl or 15 mM KCl), changes in membrane potential measured in current-clamp allowed to
330 determine the time to change completely the solution around the patched-cells (Le Guennec &
331 Noble, 1994). A complete change of the bath solution around the patched-cell occurred in less
332 than 15 secondes.
333 Whole-cell recording : the bath solution consisted of (in mM): 150 NaCl, 5 KCl, 3 $MgCl_2$, 1
334 $CaCl_2$ and 10 HEPES pH adjusted to 7.4 with NaOH. The pipette solution consisted of (in
335 mM): 155 KCl, 3 $MgCl_2$, 5 EGTA and 10 HEPES, pH adjusted to 7.2 with KOH. Cells were
336 clamped at a holding potential of -80 mV and superfused with the bath solution for over 1 min
337 before the initial current (I_0) recording. Cells were hyperpolarized to -100 mV for 50 ms and
338 then the macroscopic outward TREK-1 current ($_{I_{TREK-1}}$) was elicited with an 800 ms voltage
339 ramp protocol from -100 mV to +30 mV every ten seconds (see **Fig 2A, left panel**). Thus, the
340 evolution of the current amplitude after the perfusion change was followed in real time. The
341 perfusion condition was switched at steady-state and a minimum of 3 min perfusion was
342 applied, especially when the tested FA showed no effect. Once at steady-state, the current
343 amplitude at 0 mV during the voltage ramp was measured from the average of the last 3

344 sweeps over a delta of 1 mV (-0,5 mV to 0,5 mV). Current amplitudes are expressed in
345 current densities (pA/pF) to reduce the variability due to cell size.
346 Inside-out configuration: bath solution contained (in mM) : 140 NaCl, 4.8 KCl, 1.2 $MgCl_2$, 10
347 glucose, 10 HEPES, pH adjusted to 7.4 with NaOH. After excising the membrane patch, the
348 bath solution was replaced by the a solution identical to the pipette solution consisted of
349 (mM): 145 KCl, 1.2 $MgCl_2$, 10 glucose, 10 HEPES, pH adjusted to 7.2 with KOH. Cells were
350 clamped at a holding potential of 0 mV, the theorical equilibrium potential for K^+ ions in this
351 condition. The amplitude current was followed at +30 mV in real time during the perfusion of
352 compounds and the washout.
353
354 **Chemicals**
355 In this study we tested one direct activator of TREK-1, ML402, one saturated fatty acid,
356 stearic acid (SA), one monounsaturated fatty acid Oleic acid (OA) and 8 different PUFAs
357 (linoleic acid, LA; n-3 eicosatetraenoic acid, ETA n-3; arachidonic acid, ETA n-6; alpha-
358 linolenic acid, ALA; eicosapentaenoic acid, EPA; docosahexaenoic acid, DHA; n-3
359 docosapentaenoic acid, DPA-n3; n-6 docosapentaenoic acid, DPA-n6) having between 18 and
360 22 carbons and 2 to 6 double bonds (**Fig 1**). All reagents are summarized in the reagents and
361 tools table.
362 10 mM stock solutions were prepared by dissolving PUFAs in absolute ethanol and ML402 in
363 DMSO and stored at -80 °C to avoid PUFAs oxidation. 10 µM solutions were obtained by
364 diluting an aliquot of stock solution in the bath solution just before use for WCR experiments.
365 Cells for current recordings were first superfused with bath solution containing ethanol at
366 1/1000 as a control.

Reagent/resource	Reference or source	Identifier or catalog number
Experimental model		

HEK-293 hTREK-1 cell line	(Moha ou Maati *et al*, 2011)	
Cell culture		
DMEM + Glutamax	ThermoFisher	31966-021
Fetal bovine serum	Sigma-Aldrich	F7524-500ML
Penicilin Streptomycin	ThermoFisher	15140-122
Trypsin-EDTA	ThermoFisher	25300-054
G418 (geneticin)	Sigma-Aldrich	4727878001
Tissue culture flasks 25	TPP	90025
Tissue culture dish 35 x 10 mm	Fisher Scientific	353001
Chemicals		
Linoleic acid	Sigma-Aldrich	L1376-500MG
Oleic acid	Sigma-Aldrich	O1008-1G
Stearic acid	Sigma-Aldrich	S4751-1G
Cis-5,8,11,14,17-Eicosapentaenoic acid	Sigma-Aldrich	E2011-10MG
Cis-4,7,10,13,16,19-Docosahexaenoic acid	Sigma-Aldrich	D2534-100MG
Alpha-linolenic acid	Sigma-Aldrich	L-039-1ML
Docosapentaenoic acid (cis-7,10,13,16,19)	Sigma-Aldrich	D-120-1ML
Cis-4,7,10,13,16-Docosapentaenoic acid	Sigma-Aldrich	18566-10MG
Arachidonic acid	Sigma-Aldrich	A36-11-100MG
Omega-3 Arachidonic acid	Santa Cruz	sc229695
ML402	MedChemExpress	HY-104027
Dimethyl sulfoxide	Sigma-Aldrich	D2438
Ethanol absolute	Carlo Erba	524125
Material		
Peristaltic pump	ISMATEC	
Capillary tubes	VITREX	160214
Software		
GraphPad Prism 9	www.graphpad.com	
Clampex 10.7		
Clampfit 10.7		

367

Activation kinetics analysis

To smooth activation of TREK-1 curves with PUFAs and ML402, we used a moving average of 5 successive currents and fited it with a sigmoidal equation $I_t = I_0 + \frac{(I_{PUFA} - I_0)}{1 + e^{\frac{t_{50} - t}{\tau}}}$ (Ziaunys *et al*, 2021).

Statistical analysis

Data are presented as mean + SEM on column bar graph, and n represent the number of individual cells. All set of experiments were performed on at least three different batches (congelation and/or passage) of cells. Boxplot show the median values while the whiskers show minimal and maximal values. All descriptive statistics are displayed from Table 1 to Table 6. Statistical analysis were performed using Prism software (GraphPad Prism 9, Inc., USA). A p-value of 0.05 or less was considered as statistically significant. Kruskal-Wallis test followed by a *post hoc* Dunn's test was used for multiple comparison. The differences between groups are displayed by the letter code, where groups that do not share the same letter are significantly different.

AUTHORS CONTRIBUTION

EB carried out the experiments (WCR and IO), set up experiments and protocols, conceived the original idea and wrote the manuscript.
EA carried out the experiments (WCR) and discussed the results.
JB carried out the experiments (WCR) and discussed the results.
JL carried out the experiments(WCR) and discussed the results.
XB carried out the experiments (IO) and discussed the results.
AE drew PUFAs in **Fig 1**
CV helped supervise the project on chemistry of PUFAs and discussed the results.
TD helped supervise the project on chemistry of PUFAs and discussed the results.
JMG helped supervise the project on chemistry of PUFAs and discussed the results.
CO helped supervise the project on chemistry of PUFAs and discussed the results.
JYL set up experiments and protocols, conceived the original idea, wrote the manuscript and supervised the project.
MD set up experiments and protocols, conceived the original idea, wrote the manuscript and supervised the project.

ACKNOWLEDGEMENT

This work is supported by the Agence Nationale de la Recherche : acronym TA-BOOm (ANR-20-CE44-0001), Région Occitanie Pyrénées-Méditerranée (MNE-AGPI03), Key Initiative Montpellier Université d'Excellence (KIM Biomarkers and Therapies) and the CBS2 doctoral school. The cell line was provided by Hamid Moha ou Maati (Moha ou Maati *et al*, 2011).

REFERENCES

Bang H, Kim Y & Kim D (2000) TREK-2, a new member of the mechanosensitive tandem-pore K+ channel family. *J Biol Chem* 275: 17412–17419

Barnard ND, Goldman DM, Loomis JF, Kahleova H, Levin SM, Neabore S & Batts TC (2019) Plant-Based Diets for Cardiovascular Safety and Performance in Endurance Sports. *Nutrients* 11: E130

Danthi S, Enyeart JA & Enyeart JJ (2003) Modulation of native TREK-1 and Kv1.4 K+ channels by polyunsaturated fatty acids and lysophospholipids. *J Membr Biol* 195: 147–164

Decher N, Ortiz-Bonnin B, Friedrich C, Schewe M, Kiper AK, Rinné S, Seemann G, Peyronnet R, Zumhagen S, Bustos D, *et al* (2017) Sodium permeable and 'hypersensitive' TREK-1 channels cause ventricular tachycardia. *EMBO Mol Med* 9: 403–414

Djillani A, Mazella J, Heurteaux C & Borsotto M (2019) Role of TREK-1 in Health and Disease, Focus on the Central Nervous System. *Front Pharmacol* 10: 379

Dong YY, Pike ACW, Mackenzie A, McClenaghan C, Aryal P, Dong L, Quigley A, Grieben M, Goubin S, Mukhopadhyay S, *et al* (2015) K2P channel gating mechanisms revealed by structures of TREK-2 and a complex with Prozac. *Science* 347: 1256–1259

Fink M, Duprat F, Lesage F, Reyes R, Romey G, Heurteaux C & Lazdunski M (1996) Cloning, functional expression and brain localization of a novel unconventional outward rectifier K+ channel. *EMBO J* 15: 6854–6862

Fink M, Lesage F, Duprat F, Heurteaux C, Reyes R, Fosset M & Lazdunski M (1998) A neuronal two P domain K+ channel stimulated by arachidonic acid and polyunsaturated fatty acids. *EMBO J* 17: 3297–3308

Heurteaux C, Guy N, Laigle C, Blondeau N, Duprat F, Mazzuca M, Lang-Lazdunski L, Widmann C, Zanzouri M, Romey G, *et al* (2004) TREK-1, a K+ channel involved in neuroprotection and general anesthesia. *EMBO J* 23: 2684–2695

Honoré E (2007) The neuronal background K2P channels: focus on TREK1. *Nat Rev Neurosci* 8: 251–261

Kamatham S, Waters CM, Schwingshackl A & Mancarella S (2019) TREK-1 protects the heart against ischemia-reperfusion-induced injury and from adverse remodeling after myocardial infarction. *Pflugers Arch* 471: 1263–1272

Kang JX & Leaf A (1994) Effects of long-chain polyunsaturated fatty acids on the contraction of neonatal rat cardiac myocytes. *Proc Natl Acad Sci U S A* 91: 9886–9890

Kang JX & Leaf A (1996) Evidence that free polyunsaturated fatty acids modify Na+ channels by directly binding to the channel proteins. *Proc Natl Acad Sci U S A* 93: 3542–3546

Kelly D, Mackenzie L, Hunter P, Smaill B & Saint DA (2006) Gene expression of stretch-activated channels and mechanoelectric feedback in the heart. *Clin Exp Pharmacol Physiol* 33: 642–648

Koh SD, Monaghan K, Sergeant GP, Ro S, Walker RL, Sanders KM & Horowitz B (2001) TREK-1 regulation by nitric oxide and cGMP-dependent protein kinase. An essential role in smooth muscle inhibitory neurotransmission. *J Biol Chem* 276: 44338–44346

Lamas JA & Fernández-Fernández D (2019) Tandem pore TWIK-related potassium channels and neuroprotection. *Neural Regen Res* 14: 1293–1308

Le Guennec JV & Noble D (1994) Effects of rapid changes of external Na+ concentration at different moments during the action potential in guinea-pig myocytes. *J Physiol* 478 Pt 3: 493–504

Leifert WR, McMurchie EJ & Saint DA (1999) Inhibition of cardiac sodium currents in adult rat myocytes by n-3 polyunsaturated fatty acids. *J Physiol* 520 Pt 3: 671–679

Lesage F, Terrenoire C, Romey G & Lazdunski M (2000) Human TREK2, a 2P domain

mechano-sensitive K+ channel with multiple regulations by polyunsaturated fatty acids, lysophospholipids, and Gs, Gi, and Gq protein-coupled receptors. *J Biol Chem* 275: 28398–28405

Li X-Y & Toyoda H (2015) Role of leak potassium channels in pain signaling. *Brain Res Bull* 119: 73–79

Lolicato M, Arrigoni C, Mori T, Sekioka Y, Bryant C, Clark KA & Minor DL (2017) K2P2.1 (TREK-1)-activator complexes reveal a cryptic selectivity filter binding site. *Nature* 547: 364–368

de Lorgeril M, Renaud S, Mamelle N, Salen P, Martin JL, Monjaud I, Guidollet J, Touboul P & Delaye J (1994) Mediterranean alpha-linolenic acid-rich diet in secondary prevention of coronary heart disease. *Lancet Lond Engl* 343: 1454–1459

Ma R & Lewis A (2020) Spadin Selectively Antagonizes Arachidonic Acid Activation of TREK-1 Channels. *Front Pharmacol* 11: 434

Maingret F, Fosset M, Lesage F, Lazdunski M & Honoré E (1999) TRAAK is a mammalian neuronal mechano-gated K+ channel. *J Biol Chem* 274: 1381–1387

Maingret F, Patel AJ, Lesage F, Lazdunski M & Honoré E (2000) Lysophospholipids open the two-pore domain mechano-gated K(+) channels TREK-1 and TRAAK. *J Biol Chem* 275: 10128–10133

Mantegazza M, Rusconi R, Scalmani P, Avanzini G & Franceschetti S (2010) Epileptogenic ion channel mutations: from bedside to bench and, hopefully, back again. *Epilepsy Res* 92: 1–29

Martinac B, Zhu H, Kubalski A, Zhou XL, Culbertson M, Bussey H & Kung C (1990) Yeast K1 killer toxin forms ion channels in sensitive yeast spheroplasts and in artificial liposomes. *Proc Natl Acad Sci U S A* 87: 6228–6232

Moha ou Maati H, Peyronnet R, Devader C, Veyssiere J, Labbal F, Gandin C, Mazella J, Heurteaux C & Borsotto M (2011) A human TREK-1/HEK cell line: a highly efficient screening tool for drug development in neurological diseases. *PloS One* 6: e25602

Murbartián J, Lei Q, Sando JJ & Bayliss DA (2005) Sequential phosphorylation mediates receptor- and kinase-induced inhibition of TREK-1 background potassium channels. *J Biol Chem* 280: 30175–30184

Patel AJ, Honoré E, Maingret F, Lesage F, Fink M, Duprat F & Lazdunski M (1998) A mammalian two pore domain mechano-gated S-like K+ channel. *EMBO J* 17: 4283–4290

Patel AJ, Lazdunski M & Honoré E (2001) Lipid and mechano-gated 2P domain K(+) channels. *Curr Opin Cell Biol* 13: 422–428

Sheetz MP & Singer SJ (1974) Biological membranes as bilayer couples. A molecular mechanism of drug-erythrocyte interactions. *Proc Natl Acad Sci U S A* 71: 4457–4461

Siscovick DS, Barringer TA, Fretts AM, Wu JHY, Lichtenstein AH, Costello RB, Kris-Etherton PM, Jacobson TA, Engler MB, Alger HM, *et al* (2017) Omega-3 Polyunsaturated Fatty Acid (Fish Oil) Supplementation and the Prevention of Clinical Cardiovascular Disease: A Science Advisory From the American Heart Association. *Circulation* 135: e867–e884

Xian Tao Li null, Dyachenko V, Zuzarte M, Putzke C, Preisig-Müller R, Isenberg G & Daut J (2006) The stretch-activated potassium channel TREK-1 in rat cardiac ventricular muscle. *Cardiovasc Res* 69: 86–97

Ziaunys M, Sakalauskas A, Mikalauskaite K, Snieckute R & Smirnovas V (2021) Temperature-Dependent Structural Variability of Prion Protein Amyloid Fibrils. *Int J Mol Sci* 22: 5075

FIGURE LEGENDS

Figure 1: PUFAs and ML402 structures
Linear structures of the polyunsaturated fatty acids tested on TREK-1 activity, from the shortest acyl-chain (LA; C18) to the longest acyl-chain (DPA n-6, DPA n-3, DHA; C22).

Figure 2: Activation of TREK-1 channel by Poly-Unsaturated Fatty Acids.
A. Illustration of voltage protocol used to record I_{TREK-1}. A representative trace of current recordings during DHA application is shown in one trace *per* 10s (middle). The inset on the right shows the initial current (I_0: initial current density). **B.** Effects of different PUFAs from C18:2n-6 to C22:6n-3 on I_{TREK-1} at 0 mV. Comparison of the effects in **C.** n-3 series and **D.** n-6 series. Activations are presented as the mean + SEM fold-increase (I_{PUFA}/I_0). Descriptive statistics are given in Table I. Groups were compared with a Kruskal-Wallis test followed with the *post-hoc* Dunn's test. Two bars having the same letter are not significantly different.

Figure 3: Variability of TREK-1 activation induced by PUFAs
A. Boxplot of the fold increase (I_{PUFA}/I_0 and I_{ML402}/I_0) of TREK-1 current density at 0 mV for each PUFAs and ML402. **B**. Boxplot of the current density at steady-state (I_{PUFA} and I_{ML402}). **C.** Changes in the coefficient of variation (SD/mean) between I_{PUFA}/I_0 and current density at 0 mV. (▭ : coefficient of variation for I_{PUFA}/I_0; ▭ : coefficient of variation for I_{PUFA}). Both coefficient of variation are superimposed. Boxplots represent the median (line) with max and min values (error bar). Groups were compared with a Kruskal-Wallis test followed with the *post-hoc* Dunn's test. Two bars having the same letter are not significantly different. Descriptive statistics are given in Table 2.

Figure 4: Variability in TREK-1 activation by PUFAs depends on the initial current I_0.
A. Scatter plots representation of I_{PUFA}/I_0 as a function of I_0. **B.** Linearization of the I_{PUFA}/I_0 *vs* I_0 relationship following log-transformation for all PUFAs and ML402. The simple linear regressions (▬) are represented with the 90% confidence interval (IC;·····) used to discard one of the ETA n-3 and ETA n-6 data points (⊠). A point is discarded only if it is out by more than twice the 90% IC. Statistical analysis are given in Table 3.

Figure 5: Kinetics of activation of I_{TREK-1} by PUFAs.
A. Time course plots showing the effects of PUFAs and ML402 on I_{TREK-1} at 0mV. Kinetics were fitted with a moving average of 5 successive currents. *Insets* show the representative current densities recorded in control solution and then under PUFAs or ML402 application. PUFAs and ML402 were superfused until the steady-state was reached. Dotted lines indicate the half-time of activation. **B.** Bar graphs of the activation rate + SEM to reach the steady-state of PUFAs-activated I_{TREK-1}. Groups were compared with a Kruskal-Wallis test followed with the *post-hoc* Dunn's test. Two bars having the same letter are not significantly different. Descriptive statistics are given in Table 4.

561
562 **Figure 6: Washout kinetics of LA, EPA, DHA and ML402.**
563 **A.** Time course plots illustrating the kinetics of washing with bath solution after compounds
564 application. The current was normalized as $(I-I_0)/(I_{PUFA}-I_0)$. The first three points indicate the
565 steady-state normalized. **B.** Representation of the washout current density with a trace per
566 minute. **C.** Normalized current-time curve representing the mean ± SEM washing time for
567 each compound. Descriptive statistics are given in Table 5.
568
569
570 **Figure 7: Activation by DHA, LA and ML402 and washout kinetics of I_{TREK-1} in inside-**
571 **out configuration.**
572 Membrane potential was held at +30 mV. Activation and washout kinetics for **A.** ML402 10
573 µM **B.** LA 5 µM and **C.** DHA 5 µM superfused at the inner face of the membrane. The
574 expanded current traces where extracted at the time indicated by the arrows.. Descriptive
575 statistics are given in Table 6.
576
577
578

579

		n	Mean	SEM	SD	95 % CI	
						Lower	Upper
SA	**C18:0**	4	1	0.13	0.26	0.57	1.41
OA	**C18:1 n-9**	12	7.43	1.90	6.58	3.26	11.61
LA	**C18:2 n-6**	20	24.76	3.33	15.26	17.81	31.70
ALA	**C18:3 n-3**	12	1.36	0.11	0.38	1.12	1.60
ETA n-3	**C20:4 n-3**	12	10.93	2.01	7.24	6.56	15.53
ETA n-6	**C20:4 n-6**	16	15.66	2.13	8.78	11.14	20.17
EPA	**C20:5 n-3**	17	17.40	2.76	11.40	11.54	23.26
DPA n-6	**C22:5 n-6**	11	26.13	8.25	27.35	7.76	44.50
DPA n-3	**C22:5 n-3**	12	13.25	2.98	10.33	6.68	19.81
DHA	**C22:6 n-3**	20	29.79	4.37	19.53	20.65	38.93
ML402		19	9.56	0.98	4.25	7.51	11.61

580 **Table 1: Descriptive statistics for the current fold-increase induced by fatty acids**
581 **(I_{PUFA}/I_0) and ML402 (I_{ML402}/I_0) at 0 mV.**
582
583
584
585
586
587
588
589

590

					95 % CI	
		Mean	SEM	SD	Lower	Upper
SA	**C18:0**	18.42	5.55	11.09	0.77	36.07
OA	**C18:1 n-9**	113.1	24.61	85.27	58.91	167.3
LA	**C18:2 n-6**	353.7	22.38	102.6	307	400.4
ALA	**C18:3 n-3**	20.72	4.24	14.69	11.39	30.06
ETA n-3	**C20:4 n-3**	119.2	15.45	55.72	85.50	152.8
ETA n-6	**C20:4 n-6**	199.5	23.08	95.17	150.5	248.4
EPA	**C20:5 n-3**	211.7	21.03	86.71	167.1	256.3
DPA n-6	**C22:5 n-6**	245.3	21.41	71.00	197.6	292.9
DPA n-3	**C22:5 n-3**	147.1	26.56	92.00	88.66	205.6
DHA	**C22:6 n-3**	276.8	24.49	109.5	225.5	328.0
ML402		98.80	17.99	78.42	61.00	136.6

591 **Table 2: Descriptive statistics for the maximal current (I_{PUFA}) induced by fatty acids and**
592 **ML402.** Values indicate the current density (pA/pF) at 0 mV.
593
594

	n	p-value	R^2	Equation	Y-intercept	SD
LA	20	<0.0001	0.82	Y = -0.93*X + 2.32	2.32	0.13
ETA n-3	12	<0.0001	0.80	Y = -0.63*X + 1.67	1.67	0.12
ETA n-6	16	0.0023	0.50	Y = -0.83*X + 2.08	2.08	0.26
EPA	17	0.0008	0.53	Y = -0.72*X + 1.96	1.96	0.20
DPA n-6	11	<0.0001	0.84	Y = -1.07*X + 2.46	2.46	0.18
DPA n-3	12	0.3712	0.08	Y = -0.32*X + 1.38	1.38	0.37
DHA	20	<0.0001	0.68	Y = -0.74*X + 2.13	2.13	0.13
ML402	19	0.8627	0.00	Y = -0.03*X + 0.96	0.96	0.18

595 **Table 3: Parameters of the linear regression Log10 (I_{PUFA}/I_0)=f(Log10(I_0)) for PUFAs**
596 **and ML402.**
597
598

		Half-activation (min)			Time constant (min)		Activation rate (min-1)		
	n	Mean	SEM		Mean	SEM	Mean	SEM	
LA	20	1.86	0.16	a	0.38	0.07	4.50	0.68	a
ETA n-3	12	4.55	0.25	b	1.29	0.14	0.87	0.08	b
ETA n-6	16	3.96	0.31	b	1.24	0.28	1.07	0.09	b
EPA	17	3.17	0.30	bc	0.60	0.06	2.01	0.26	a
DPA n-6	11	3.11	0.30	bd	0.77	0.12	1.54	0.17	ab
DPA n-3	12	4.17	0.35	b	1.10	0.10	0.99	0.09	b
DHA	20	2.26	0.18	ac	0.37	0.04	3.39	0.39	a
ML402	19	2.10	0.16	acd	0.47	0.13	3.66	0.49	a

Table 4: Descriptive statistics for activation kinetics of TREK-1 by PUFAs and ML402. Values indicate the time (min) needed to reach the half-activation of the TREK-1 activation. Time constant (min) derived from the sigmoidal fit and activation rate (min^{-1}) was calculated as : $\frac{1}{Time\ constant}$. Two FA having the same letter are not significantly different.

		10%		20%		30%		40%		50%	
		Mean	SEM	Mean	SEM	Mean	SEM	Mean	SEM	Mean	SEM
LA	**C18:2 n-6**	0.67	0.19	1.22	0.36	1.67	0.43	2.02	0.51	2.5	0.63
EPA	**C20:5 n-3**	0.37	0.06	0.6	0.08	0.73	0.083	0.86	0.07	1	0.08
DHA	**C22:6 n-3**	1.03	0.14	1.7	0.18	2.36	0.23	2.99	0.27	3.82	0.37
ML402		0.04	0.018	0.18	0.03	0.33	0.031	0.43	0.04	0.57	0.04

Table 5: Descriptive statistics for washout kinetics in WCR configuration. Values indicate the time (min) needed to reach the indicated % of washout.

		Steady-state (min)		50 % washout (s)	
	n	Mean	SEM	Mean	SEM
LA	4	4.58	0.39	18.25	6.33
DHA	6	2.92	0.27	18.25	4.19
ML402	6	2.56	0.56	15.50	7.56

Table 6: **Descriptive statistics for TREK-1 activation kinetic and washout in inside-out configuration.** Values indicate the time needed to reach the steady-state (min) and the time to reach 50% of washout (s).

LA	Linoleic acid	C18:2 n-6	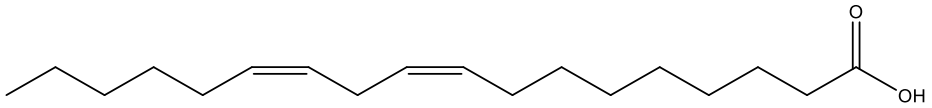
ALA	Alpha-linolenic acid	C18:3 n-3	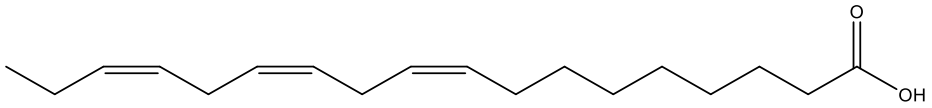
ETA n-3	Eicosatetraenoic acid n-3	C20:4 n-3	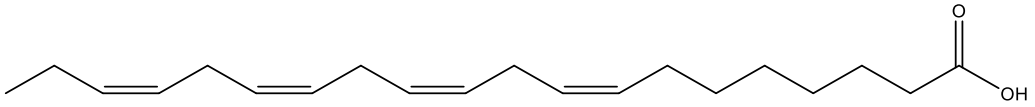
ETA n-6	Eicosatetraenoic acid n-6	C20:4 n-6	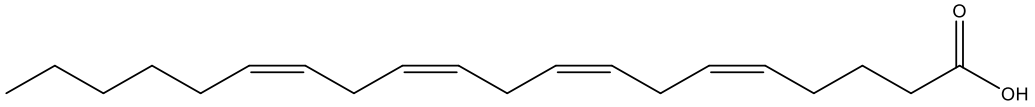
EPA	Eicosapentaenoic acid	C20:5 n-3	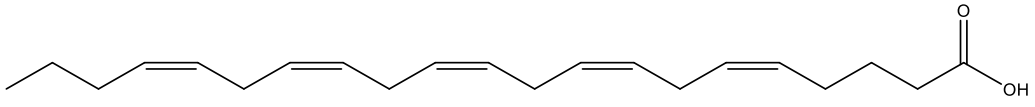
DPA n-6	Docosapentaenoic acid n-6	C22:5 n-6	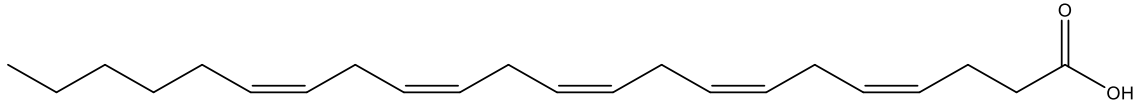
DPA n-3	Docosapentaenoic acid n-3	C22:5 n-3	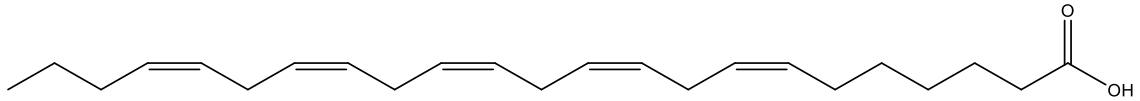
DHA	Docosahexaenoic acid	C22:6 n-3	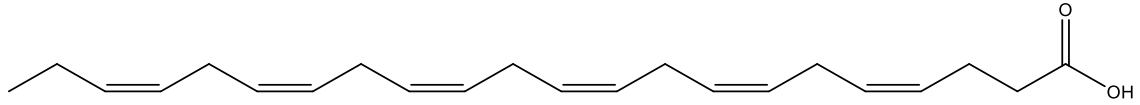
ML402			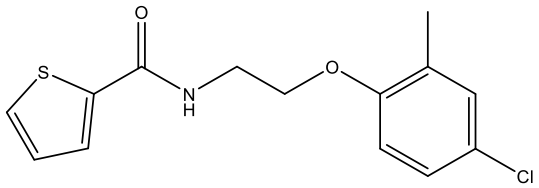

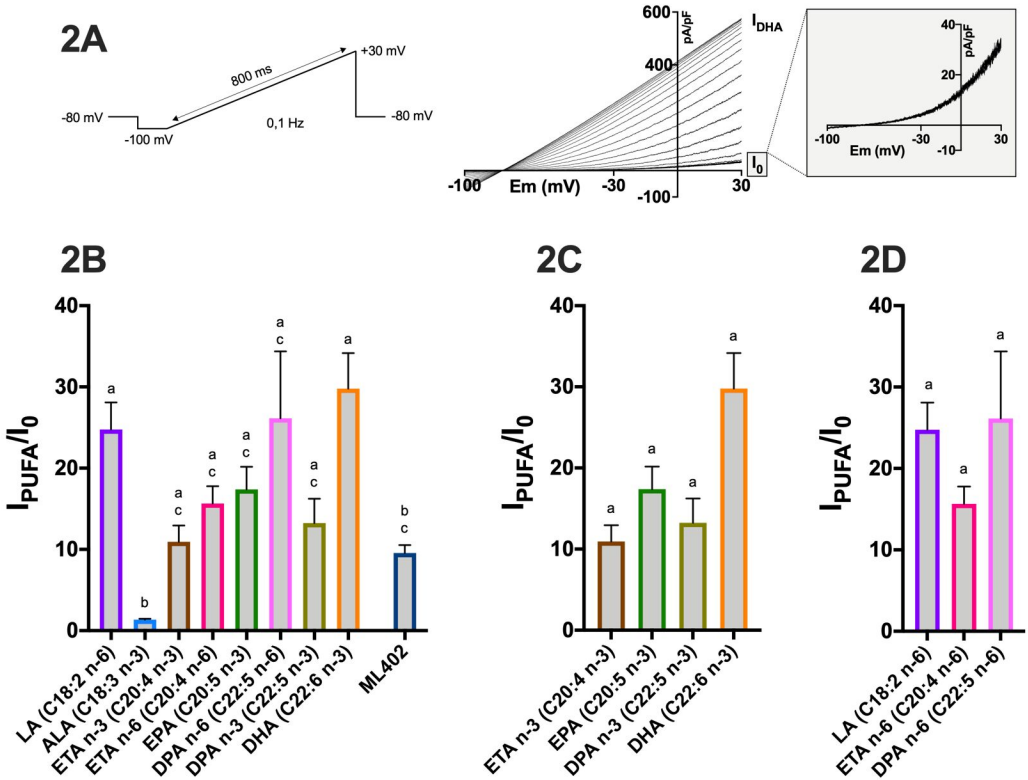
2A
-80 mV
-100 mV
800 ms
+30 mV
0,1 Hz
-80 mV
600
400
pA/pF
I DHA
I 0
-100
Em (mV)
-30
30
-100
40
20
pA/pF
-100
-30
30
Em (mV)
-10
2B
2C
2D
I PUFA/I 0
40
30
20
10
0
a
b
c
LA (C18:2 n-6)
ALA (C18:3 n-3)
ETA n-3 (C20:4 n-3)
ETA n-6 (C20:4 n-6)
EPA (C20:5 n-3)
EPA (C20:5 n-6)
DPA n-3 (C22:5 n-3)
DPA n-6 (C22:5 n-6)
DHA (C22:6 n-3)
ML402
ETA n-3 (C20:4 n-3)
EPA (C20:5 n-3)
DPA n-3 (C22:5 n-3)
DHA (C22:6 n-3)
LA (C18:2 n-6)
ETA n-6 (C20:4 n-6)
DPA n-6 (C22:5 n-6)

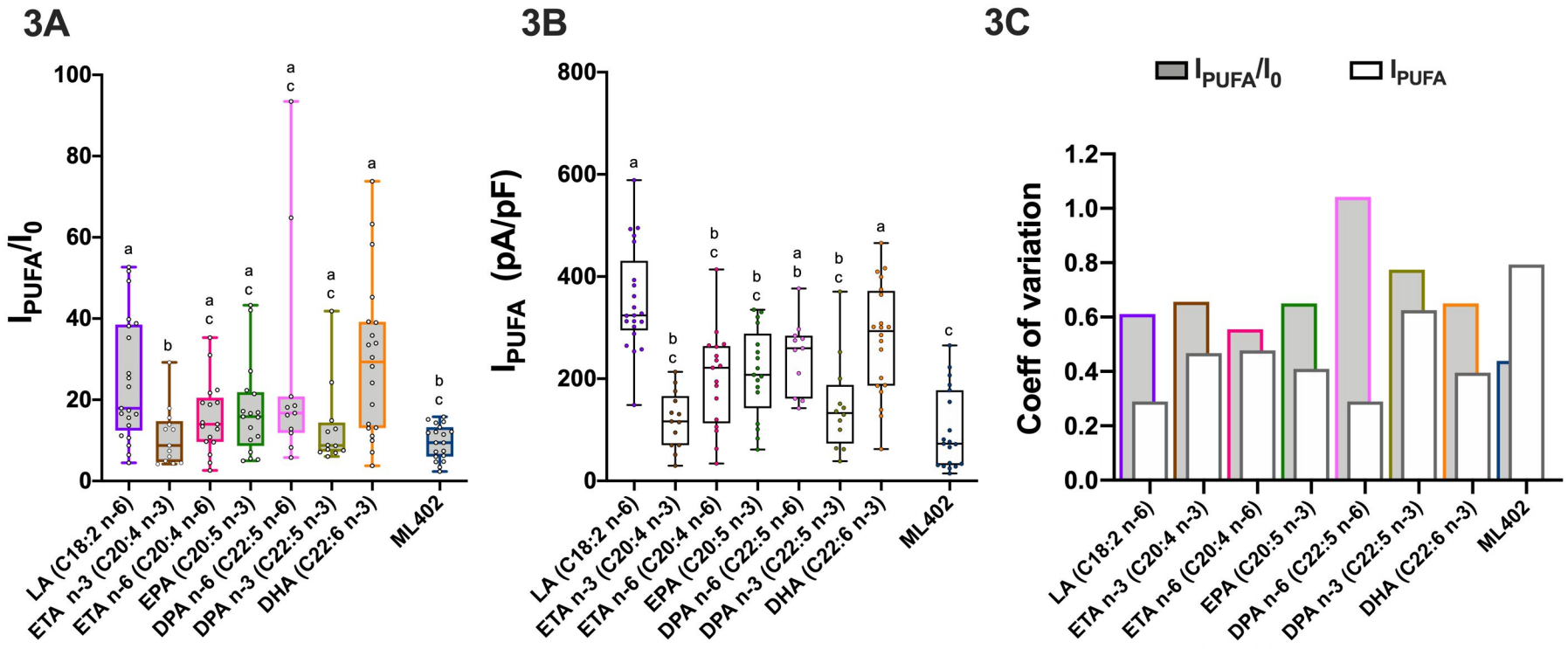
3A
3B
3C
I_{PUFA}/I_0
I_{PUFA} (pA/pF)
Coeff of variation
I_{PUFA}/I_0
I_{PUFA}
LA (C18:2 n-6)
ETA n-3 (C20:4 n-3)
ETA n-6 (C20:4 n-6)
EPA (C20:5 n-3)
DPA n-6 (C22:5 n-6)
DPA n-3 (C22:5 n-3)
DHA (C22:6 n-3)
ML402

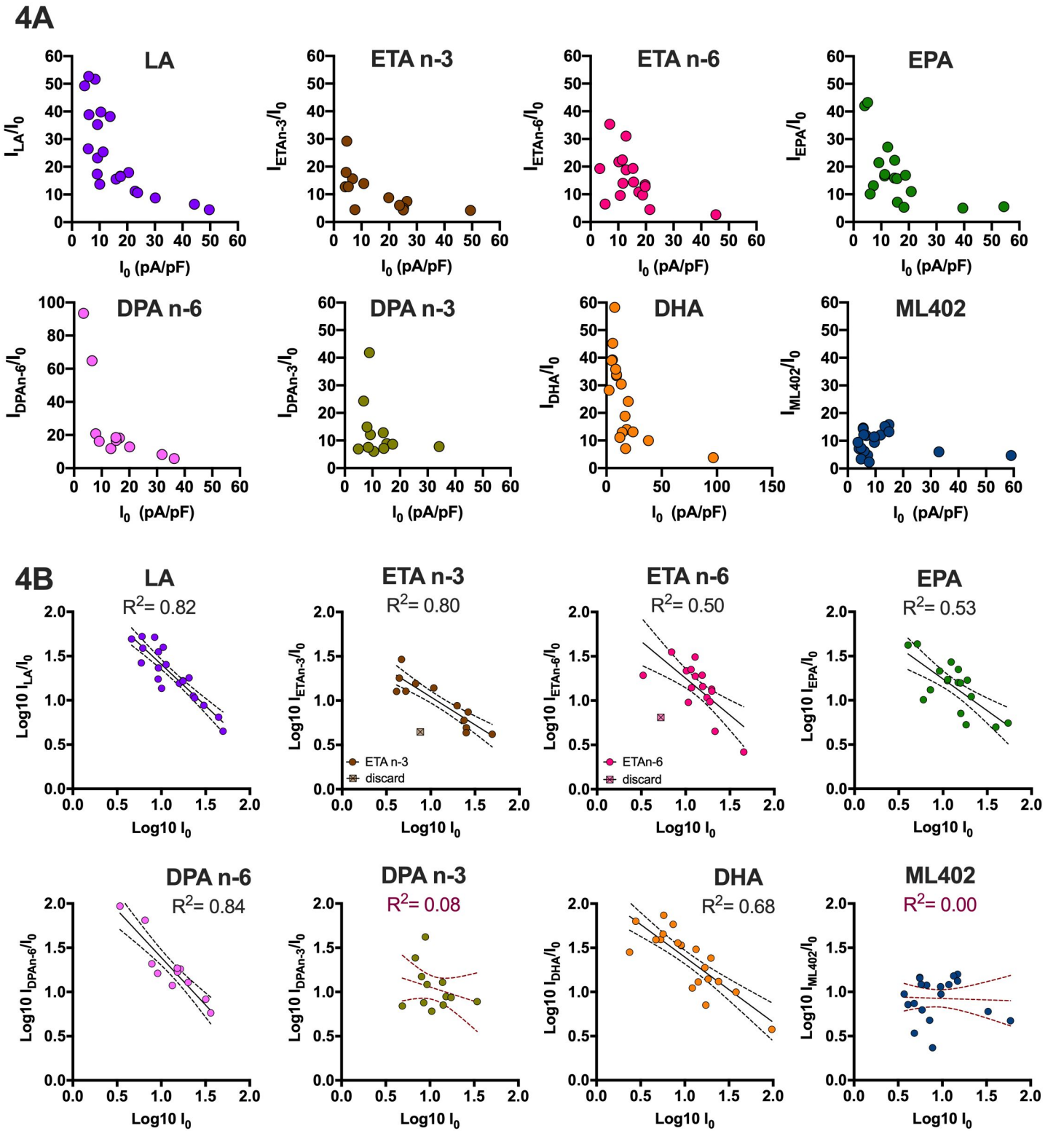
4A
LA
ETA n-3
ETA n-6
EPA
DPA n-6
DPA n-3
DHA
ML402
I_{LA}/I_0
I_{ETAn-3}/I_0
I_{ETAn-6}/I_0
I_{EPA}/I_0
I_{DPAn-6}/I_0
I_{DPAn-3}/I_0
I_{DHA}/I_0
I_{ML402}/I_0
I_0 (pA/pF)
4B
R^2= 0.82
R^2= 0.80
R^2= 0.50
R^2= 0.53
R^2= 0.84
R^2= 0.08
R^2= 0.68
R^2= 0.00
ETA n-3
discard
ETAn-6
discard
Log10 I_{LA}/I_0
Log10 I_{ETAn-3}/I_0
Log10 I_{ETAn-6}/I_0
Log10 I_{EPA}/I_0
Log10 I_{DPAn-6}/I_0
Log10 I_{DPAn-3}/I_0
Log10 I_{DHA}/I_0
Log10 I_{ML402}/I_0
Log10 I_0

5A

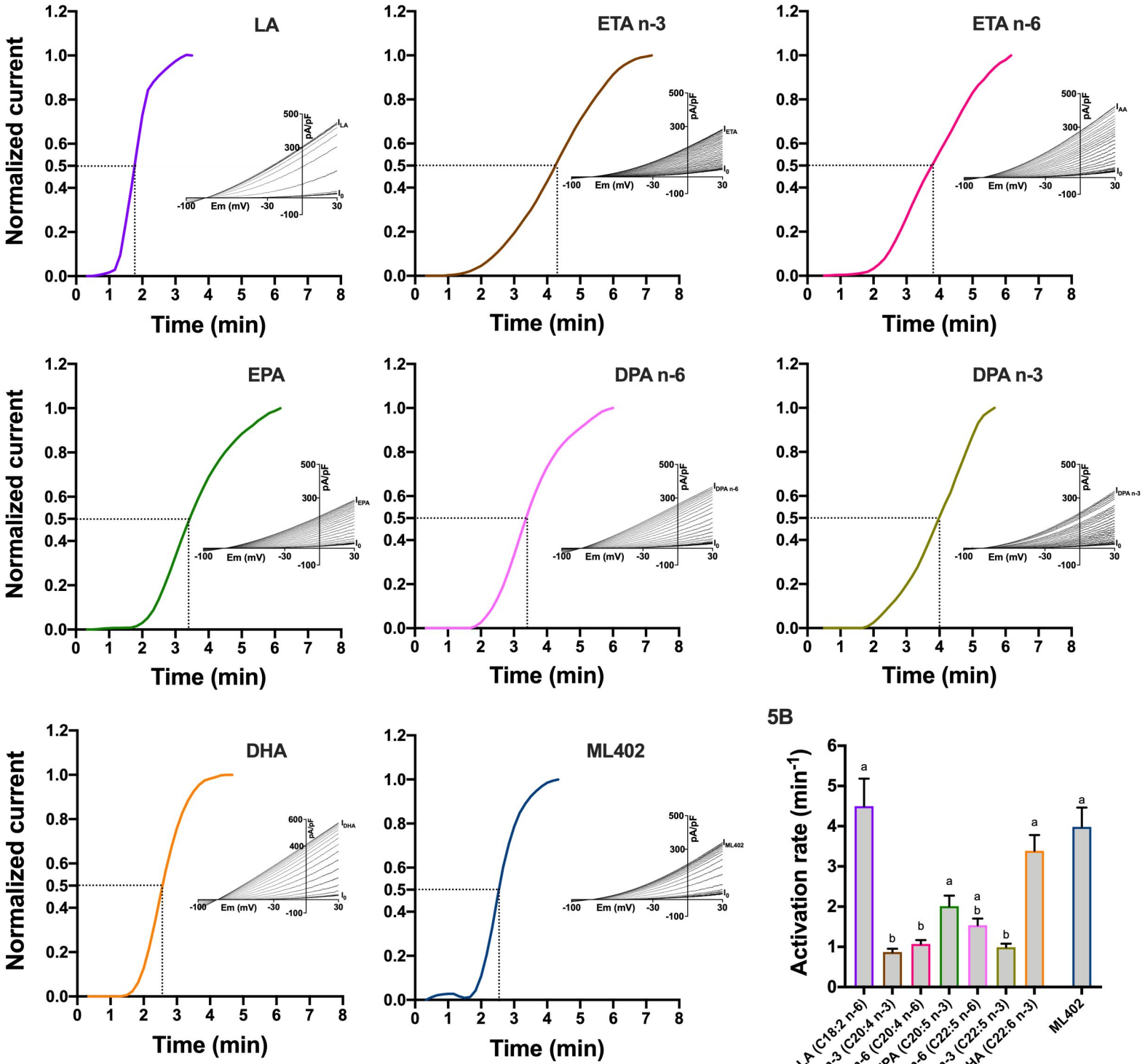
LA
ETA n-3
ETA n-6
EPA
DPA n-6
DPA n-3
DHA
ML402
Normalized current
Time (min)
pA/pF
Em (mV)
I_{LA}
I_{ETA}
I_{AA}
I_{EPA}
$I_{DPA\ n-6}$
$I_{DPA\ n-3}$
I_{DHA}
I_{ML402}
I_0

5B

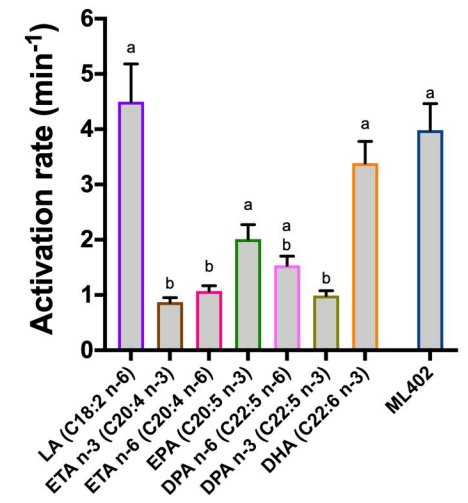
Activation rate (min^{-1})
LA (C18:2 n-6)
ETA n-3 (C20:4 n-3)
ETA n-6 (C20:4 n-6)
EPA (C20:5 n-3)
DPA n-6 (C22:5 n-6)
DPA n-3 (C22:5 n-3)
DHA (C22:6 n-3)
ML402

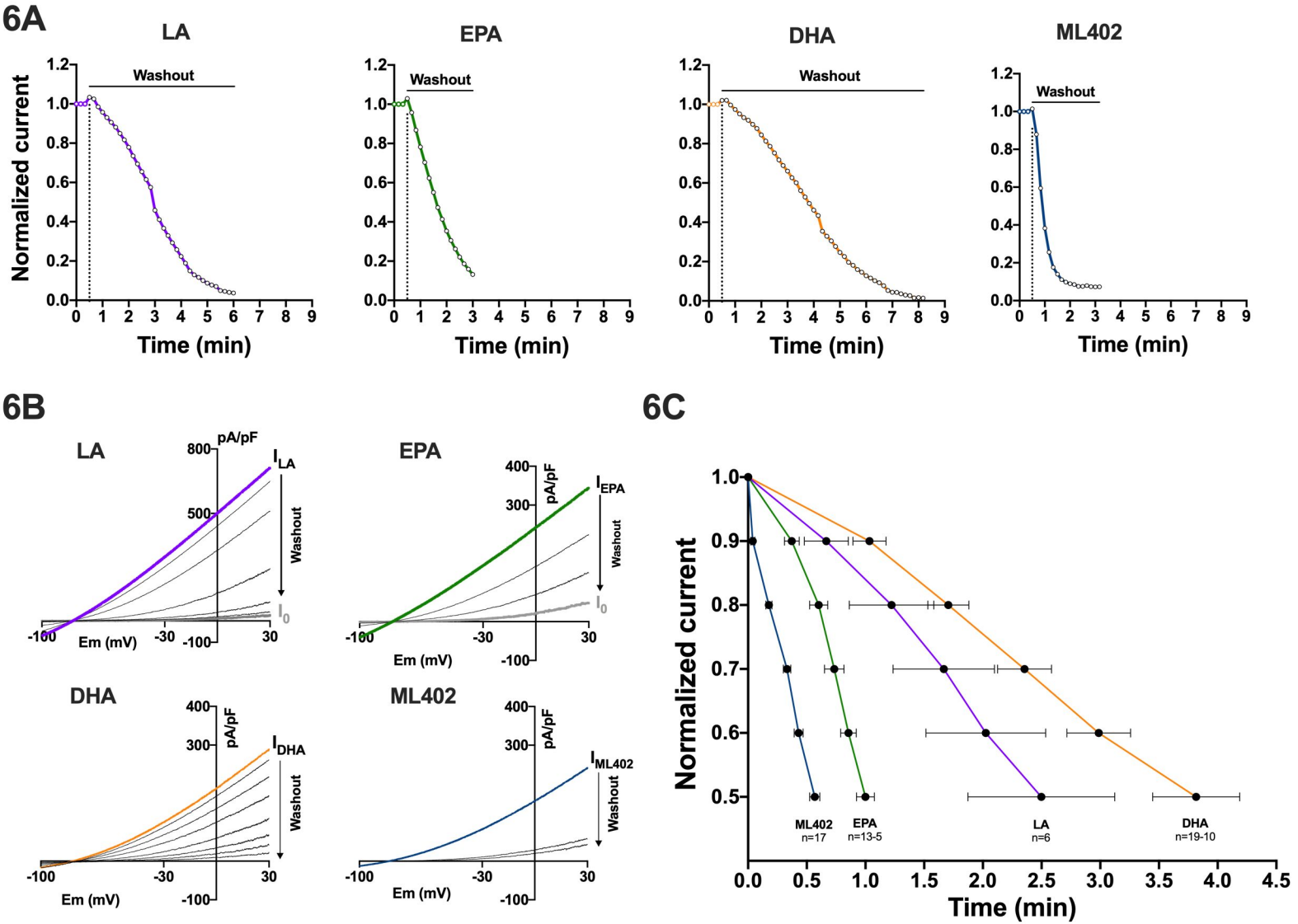
6A
LA
EPA
DHA
ML402
Washout
Normalized current
Time (min)
6B
pA/pF
Em (mV)
I_{LA}
I_{EPA}
I_{DHA}
I_{ML402}
I_0
6C
ML402
n=17
EPA
n=13-5
LA
n=6
DHA
n=19-10

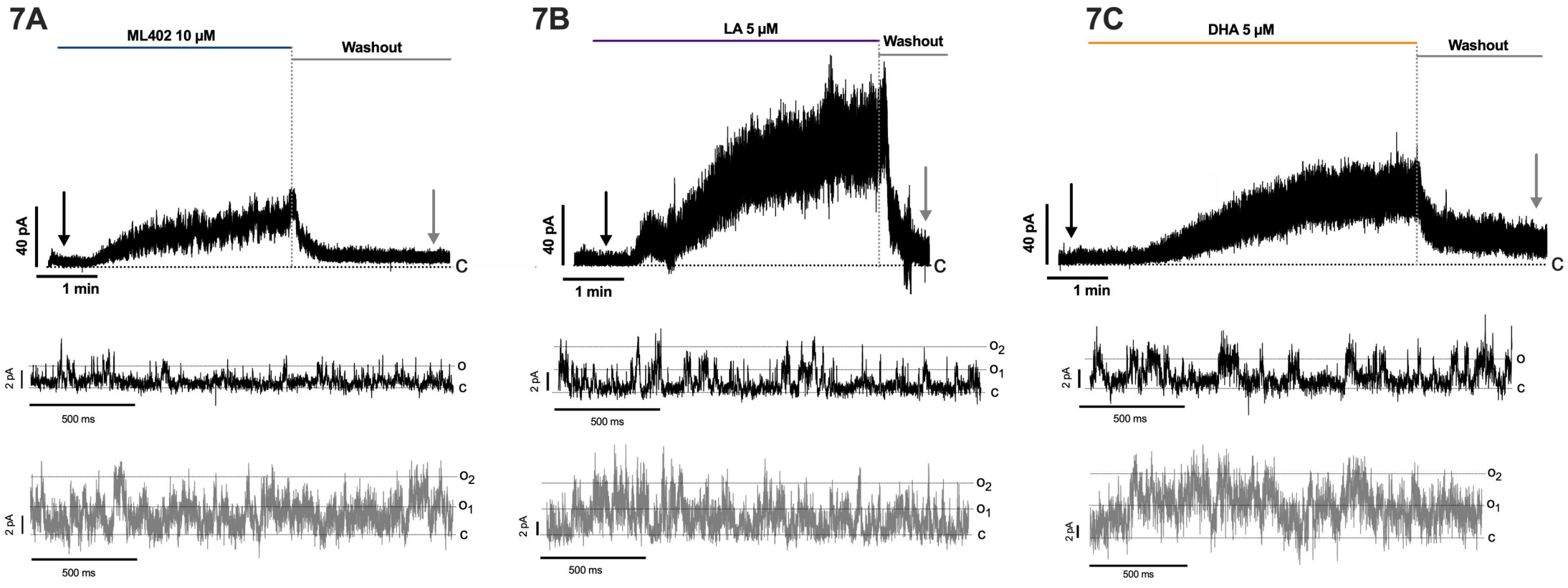
7A
ML402 10 μM
Washout
40 pA
1 min
C
2 pA
500 ms
O
C
O2
O1
C
7B
LA 5 μM
Washout
40 pA
1 min
C
2 pA
500 ms
O2
O1
C
7C
DHA 5 μM
Washout
40 pA
1 min
C
2 pA
500 ms
O
C
O2
O1
C